BILINGUAL PUBLISHING GROUP

Journal of Environmental & Earth Sciences

https://journals.bilpubgroup.com/index.php/jees

ARTICLE

Research and Application of Assessment of Wind Energy in Large-Scale Wind Power Bases

Ling Yuan [1*], Ling Bai [2,3], Jianke Li [1], Peng Chen [1], Haichuan Long [1], Xia Ruan [1], Qi Luo [2,4]

[1] *Haizhuang Wind Power Co., Ltd., China State Shipbuilding Corp. (CSSC), Chongqing 401120, China*

[2] *Economic Transformation of Climate Resources Key Laboratory, China Meteorological Administration, Chongqing 401120, China*

[3] *Liangping Meteorological Bureau, Chongqing 405200, China*

[4] *Chongqing Shete Meteorological Application Research Institute, Chongqing Meteorological Service, Chongqing 401120, China*

ABSTRACT

Improving the accuracy of the evaluation of the performance of wind farms in large wind power bases located in complex terrain under the actual atmosphere is crucial to the sustainable development of wind power. To this end, this study combined the Weather Research and Forecasting (WRF) model with the Wind Farm Parameterization (WFP) method to investigate the wake characteristics and operational performance of large onshore wind farms in the complex terrain of Jiuquan City, Gansu Province, China. The research results showed that after verification, the systematic error of the WRF simulations was less than 3%. The WRF model and the WFP scheme simulated a significant warming phenomenon within the wind power base area, while a cooling effect was observed outside. The analysis of the wake effects indicated that the impact of Phase I construction on Phase II construction of the wind power base was minimal. During the operation of the entire wind power base, the wind speed within the wind farm decreased by approximately 10%, and the influence range of the predominant wind direction extended over a hundred kilometers downwind. The research conclusions provide a powerful scientific basis for optimizing design and operation, improving efficiency, minimizing the negative impacts on adjacent wind turbines, and ensuring the sustainable development of wind energy

*CORRESPONDING AUTHOR:

Ling Yuan, Haizhuang Wind Power Co., Ltd., China State Shipbuilding Corp (CSSC), Chongqing 401120, China; Email: 18614047730@163.com

ARTICLE INFO

Received: 28 October 2024 | Revised: 17 November 2024 | Accepted: 20 November 2024 | Published Online: 23 January 2025

DOI: https://doi.org/10.30564/jees.v7i2.7620

CITATION

Yuan, L., Bai, L., Li, J., et al., 2025. Research and Application of Assessment of Wind Energy in Large-Scale Wind Power Bases. Journal of Environmental & Earth Sciences. 7(2): 117–128. DOI: https://doi.org/10.30564/jees.v7i2.7620

through dynamic planning and scientific assessment.

Keywords: Large-Scale Wind Power Base; Mesoscale Simulation; Risk Assessment; Performance Evaluation and Improvement

1. Introduction

With the continuous increase in wind farm construction, under the support of China's national policies, it has become a major trend to construct large-scale wind power bases in complex terrains with good wind resources[1]. Conducting parametric simulations of large-scale onshore wind energy bases can further evaluate the ecological environmental issues and power generation capacity of wind turbines in these areas. Due to the unique characteristics of wind power generation, the operation and efficiency of wind farms in the natural atmospheric environment are affected not only by meteorological conditions but also by the complex multi-scale interactions between wind turbines and the atmospheric boundary layer. The wake effect formed by these interactions will greatly affect the power generation revenue of wind farms[2]. Therefore, based on the accurate simulation of wind energy resources in wind farms and considering the interaction between wind turbines and the atmosphere under natural atmospheric conditions, further parametric simulation of wind farms can significantly improve the accuracy of predicting the power generation capacity of prospective wind farms, effectively reduce the risks of wind power development, and provide reliable support for scientific decision-making.

Various methods, such as in-situ observations, satellite remote sensing, wind tunnel experiments, and numerical simulations, are widely used to study this issue. Among these, observations are a suitable and direct method to explore the physics and performance of wind farm wakes under natural atmospheric conditions, using various measurement devices such as anemometers[3], LiDAR measurements[4, 5], drones[6], and satellite remote sensing[7]. These field measurements reflect the various inflow conditions specific to particular wind turbines. Wind tunnel experiments can be used to visualize the wake near wind turbines. However, most studies are based on uniform or even empirical inflow boundary conditions, which do not reflect actual atmospheric inflow conditions. Moreover, due to the limitations of testing technologies, irregular variations, randomness, and intermittency similar to absolute atmospheres may increase measurement uncertainties.

Numerical simulations can capture flow details of the target wind farm across various temporal and spatial scales. Based on the size of wind turbine arrays, numerical techniques are typically categorized into two types[8]. Research achievements in the first category primarily focus on studying individual wind turbines by resolving the Na-vier-Stokes equations. The turbulent flow around wind farms is explored using an actuator disk/line model within the Large-Eddy Simulation (LES) framework, capturing its significant impact on the boundary-layer depth[6, 9]. Additionally, modeling wind turbines as actuator lines based on blade aerodynamic parameters detects the influence of atmospheric stability and surface roughness on the dynamics of individual wind turbines[10]. Although these studies provide deep insights into the flow details within wind turbines' rotational area and wake, they are computationally expensive and time-consuming. However, applying mesoscale numerical prediction (NWP) models in evaluating large-scale wind farms is increasingly common. Among these, the Weather Research and Forecasting (WRF) model[11], an advanced atmospheric simulation system within the NWP framework, has been utilized for assessing wind farms based on realistic atmospheric process simulations. A series of studies have employed the WRF model for wind resource simulations[2, 12, 13] alongside investigations into the sensitivity of initial and boundary conditions and the physical schemes[14]. Furthermore, the WRF model can explore meteorological characteristics in regions with complex terrain by coupling with other models[13], such as microscale models.

To parameterize the impact of wind farms on the local atmosphere, wind farm parameterization (WFP) was proposed and implemented in climate models[15]. In these models, the resolved kinetic energy extracted from local conditions by wind turbines is represented as the thrust coefficient. The proper fraction of drag is transformed into electrical power, and the remainder of ineffective drag is converted into turbulence kinetic energy (TKE). The new WFP was

used to predict the tur-bine-induced forces and TKE in a hypothetical wind farm, and the results were validated through Large-Eddy Simulation (LES) analysis[16]. However, limited research couples the WRF model with the WFP method for substantial realistic wind farms in complex terrain. Onshore wind farms' flow properties and performance are influenced by atmospheric stability, wind resources (primarily wind speed and direction), and topography. Additionally, the atmospheric impacts of wind farms on local wind speeds may vary with the size of the wind farms[17] and are also influenced by terrain complexity[18].

This in-depth study is dedicated to the exploration of the wake behavior and performance of large-scale onshore wind farms within a wind power base that is situated in complex terrain. To conduct this research, the WRF model combined with the WFP method is utilized, enabling a comprehensive analysis of the intricate wind dynamics. The specific area of focus is the Jiuquan wind power base in Gansu Province, China, which presents a unique set of challenges and opportunities due to its geographical and environmental characteristics. The rest of the paper is carefully structured to present a clear and logical flow of information. In Section 2, a detailed introduction of the data and methodology is provided. This includes an in-depth look at the wind power base itself, shedding light on its layout, capacity, and other relevant features. Additionally, information regarding the various data sources used in the study is presented, ensuring transparency and reproducibility. The section also delves into the specifics of the mesoscale numerical simulation, explaining the parameters, assumptions, and techniques employed. Section 3 then focuses on model validation, which is crucial for establishing the reliability of the results. It further explores the wake behavior and performance of large-scale wind farms under different conditions, considering factors such as wind speed, direction, and variations in terrain. Finally, Section 4 succinctly summarizes the research conclusions, highlighting the key findings and their implications for the future development and operation of wind farms in similar complex terrains.

2. Materials and Methods

2.1. Study Area and Measurements

The large wind farm located in Yumen Town, Jiuquan City, Gansu Province, is the project of China's first ten-million-kilowatt wind power base. This project includes more than 10,000 wind turbines of various models from different manufacturers. The terrain of the wind farm is shown in Figure 1a. The project was constructed in two phases. Phase I was completed before 2012 (the black part in **Figure 1b**). The installed single-unit capacity of the wind turbines was less than 1.5 megawatts, with a total installed capacity of 5.16 million kilowatts. For Phase II, the construction capacity of the first batch was 3 million kilowatts (the red area in **Figure 1b**), and that of the second batch was 5 million kilowatts (the blue area in **Figure 1b**). By the end of 2022, Phase II had been fully completed. The project covers the area between 95° E and 98° E in longitude and 39.5° N and 41.5° N in latitude.

There are numerous high mountains in the north and south, while the terrain is flat and open in the east-west direction, and the wind direction is stable, which makes it suitable for the construction of a large wind power base. Meanwhile, the meteorological changes in the near-surface environment caused by the operation of the wind farm have a great impact on the revenue of the wind farm. This study takes this as the research object and analyzes the flow field changes of this large wind power base and its impact on the atmospheric boundary layer environment based on observations and combined with numerical simulation methods.

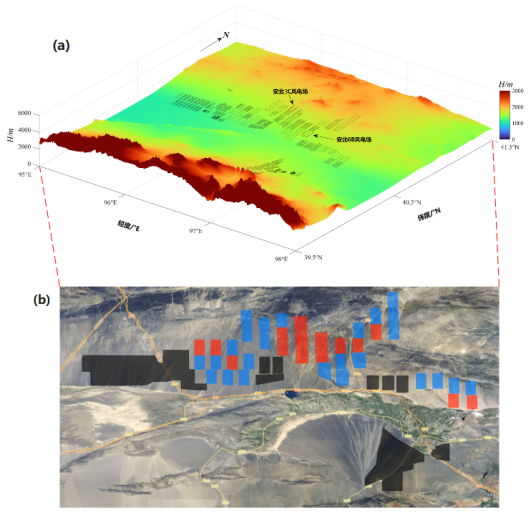

Figure 1. The maps of the study area and wind farm distribution. (**a**) The terrain of the wind farm; (**b**) The area scope of the already-built wind farm (The black area represents the phase I of the wind farm, and the red and blue areas represent the phase II).

This study collected data from a wind tower located within the Phase II wind farm of the wind power base to val-

idate the numerical simulation results. The measurement period spans from September 28, 2008, to September 21, 2014, with the location coordinates at 96.712333° E, 40.7289° N. Detailed data information is provided in **Table 1**.

Table 1. Basic information on the wind tower.

No.	Wind Tower Latitude/Longitude	Elevation	Anemometer Configuration	Period
8777#	96.712333° E 40.7289° N	1518 m	Wind speed: 70 m/50 m/30 m/10 m Wind direction: 70 m/10 m Temperature and Pressure: 7 m	2008.09.28–2014.09.21

2.2. Mesoscale Simulations

It is widely known that the mesoscale NWP model is becoming increasingly popular in the evaluation of large-scale wind farms. Currently, the WRF model, as an advanced atmospheric simulation system among numerical prediction models, can not only be used to explore the meteorological characteristics of regions with complex terrain by utilizing coupling models (such as combining the WRF model with microscale models), but also be applied to evaluate wind farms based on simulations of actual atmospheric processes. Previous studies have carried out a series of research on wind resource simulation using the WRF model [2, 12, 13], and also studied the sensitivities of the initial conditions, boundary conditions, and physical schemes of the WRF model [14].

In this study, the mesoscale numerical model WRF Version 3.7.1 is employed to simulate the wind properties and performance of the large onshore wind farms in the Jiuquan wind power base. The model initial and lateral boundary conditions are provided by the latest global reanalysis dataset from ECMWF (European Centre for Medium-Range Weather Forecasts), i.e., ERA5 [19]. **Figure 2** displays three nested domains, with the wind farms in Jiuquan located in the innermost domain (d03). Grid nudging is applied in the parent domains (d01 and d02) using four-dimensional data assimilation (FDDA) to ensure that simulation results closely match analyses and observations through coarse integration [11]. The resolution of the USGS static data in the MODIS-based land-use data is modis_30s+30s across all three domains, and the projection is set to Lambert.

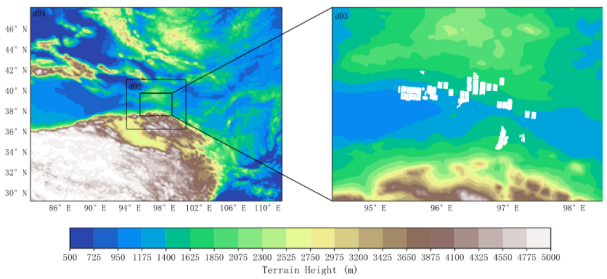

Figure 2. Domain configurations for the Jiuquan City wind farms.

Considering the topographic complexity of the study area, we design the experiment cases of horizontal resolutions $\Delta x = 1000$ m. Besides, in the vertical dimension, 81 levels are set, with the top at 20 km and 41 levels below 1 km, of which 13 levels intersect the rotor region. To accurately reflect the atmospheric process of substantial onshore wind farms in the explored region, the physics and dynamics schemes in the WRF model are configured according to the previous studies, as summarized in **Table 2**. Besides, to ensure the effective implementation of the wind farm parameterization, a planetary boundary layer physics scheme is configured as Mellor–Yamada–Janjic turbulent kinetic energy (*TKE*) [20] with Grell 3D scheme [21, 22] ensemble cumulus parameterization.

Table 2. Summary of the physics and dynamics configurations for the present WRF model.

Physics and Dynamics	Scheme
Microphysics	Modified Thompson scheme [23]
Longwave Radiation	Rapid Radiative Transfer Model (RRTM) [24]
Shortwave Radiation	Dudhia scheme [25]
Planetary boundary layer	Mellor–Yamada–Janjic turbulent kinetic energy (TKE) [20]
Cumulus parameterization	Grell 3D scheme [21, 22]
Land surface model	Unified Noah land surface model [26]
Sub-grid orographic drag	Turbulent orographic form drag scheme [27, 28]
Wind farm parameterization	Fitch's Model [29]

2.3. Parameterization Scheme of Wind Farm

This study applies a wind farm parameterization model, which assumes that the resolved kinetic energy (*RKE*) extracted by wind turbines from the ambient conditions is partially converted into electrical energy (EE) and partially into turbulence kinetic energy (*TKE*)[15, 20]. The thrust coefficient (C_T) is used to determine the *RKE*, while the power coefficient (C_P) is used to estimate the *EE*. The *TKE* is then calculated as $C_{TKE} = C_T - C_P$. In this model, it is assumed that wind turbines are oriented perpendicular to the airflow and that the drag of the wind turbine does not impact the vertical component of wind speed. Consequently, the drag force (Equation (1)) induced by a wind turbine on the atmosphere is calculated as follows:

$$F_D = \frac{1}{2} C_T \rho |U| U A \tag{1}$$

where $U = (u, v)$ represents the horizontal wind speed at the hub height of the wind turbines, ρ is the air density, C_T is the turbine thrust coefficient, and A is the rotor area, determined by the diameter (D) of the wind turbine blades. Given the non-uniform distribution of the vertical profile of the zonal and meridional wind, the kinetic energy (*KE*) loss rate (Equation (2)) from the ambient air caused by a single turbine is:

$$\frac{\partial KE_{drag}}{\partial t} = -\frac{1}{2} \int_{A_R} \rho C_T |U|^3 dA \tag{2}$$

In Cartesian coordinates, the loss rate of *KE* in a grid cell (i, j) at vertical levels intersected by turbine blades and the total change rate of KE in one grid cell (Equation (3)) is given by:

$$\begin{cases} \frac{\partial KE_{drag}^{ijk}}{\partial t} = \frac{1}{2} N_T^{ij} \int_{\Delta x} \int_{\Delta y} \left[\int_{z_k}^{z_{k+1}} C_T \rho_{ijk} |U|^3 dz \right] dxdy \\ = -\frac{1}{2} N_T^{ij} \Delta x \Delta y C_T \rho_{ijk} |U|_{ijk}^3 A_{ijk} \\ \frac{\partial KE_{cell}^{ijk}}{\partial t} = \frac{\partial}{\partial x} \int_{\Delta x} \int_{\Delta y} \int_{\Delta z} \frac{\rho_{ijk}}{2} |U|_{ijk}^2 dxdydz \\ = \rho_{ijk} |U|_{ijk} \frac{\partial |U|_{ijk}}{\partial t} (z_{k+1} - z_k) \Delta x \Delta y \end{cases} \tag{3}$$

where $N_T ij$ is the horizontal density of the number of turbines, Δx and Δy are the horizontal grid size in the zonal and meridional directions, and A_{ijk} is the cross-sectional area cut by one turbine blade between the model levels k and k+1 in a grid cell (i, j). Due to the equality of change rate of *KE* within grid cell (i, j, k) and the loss rate of *KE* suffered by wind turbines in one grid cell, the momentum tendency term (Equation (4)) is obtained from Equation (3):

$$\frac{\partial |U|_{ij}}{\partial t} = -\frac{1}{2} \frac{N_T^{ij} C_T |U|_{ij}^2 A_{ijk}}{z_{k+1} - z_k} \tag{4}$$

The total useful electrical power of wind farms and the *TKE* caused by wind farms in the atmosphere (Equation (5)) can be obtained by the following:

$$\begin{cases} P = \sum_i \sum_j \sum_{k=z_{bot}}^{k=z_{top}} \frac{1}{2} N_T^{ij} C_P \rho_{ijk} |U|_{ijk}^3 A_{ijk} \\ TKE = \sum_i \sum_j \sum_{k=z_{bot}}^{k=z_{top}} \frac{1}{2} N_T^{ij} C_{TKE} \rho_{ijk} |U|_{ijk}^3 A_{ijk} \end{cases} \tag{5}$$

Therefore, based on the wind farm parameterization method, the wake influence of the wind farms on the atmosphere can be resolved by imposing a momentum sink and turbulence source on the mean flow.

2.4. Wind Resource Simulation Experiment Setup

In this study, it is noteworthy that to estimate the wake influence of the wind farms, we designed several simulated comparative test cases (**Table 3**), including WRF simulations with and without wind farm parameterization (U_{turbo} and $U_{none-turbo}$). The specific experimental setups are as follows:

Table 3. Basic information of the experimental setups in this study.

	Study Period	Wind Tower Data	Wind Speed and Temperature Differences	Key Issues to Be Addressed
Experiment 1	2010	√	/	Testing and validating the accuracy of numerical simulation results.
Experiment 2	2013	√	$\Delta U = U_{\text{none-turbo}} - U_{\text{turbo}}$ $\Delta T = T_{\text{none-turbo}} - T_{\text{turbo}}$	Studying whether the Phase I wind farm at the wind power base affects the wind field at the 8777# wind tower location in Phase II.
Experiment 3	2022	×		Exploring the interaction between the wake effects of the entire wind power base and the atmospheric environment.

2.5. Evaluation Metrics

In this study, two crucial comparison indices were adopted to comprehensively evaluate the performance of the model simulation values (Mi) about the actual wind tower measurement values (Gi).

(1) The mean bias (*MB*) (Equation (6)), may take a positive value, which means that the simulation results are overestimated compared to the measurement values. It may also take a negative value, indicating an underestimated situation. By comparing the simulation values with the actual measurement values from the wind tower, the MB can provide valuable insights into the overall accuracy of the model's predictions in terms of (numerical) direction (that is, whether the model's predictions tend to be higher or lower than the actual values).

(2) The root mean square error (RMSE) (Equation (7)), aims to measure the variation of the simulation values concerning the measurement values. Essentially, it quantifies the average degree to which the simulation values deviate from the actual measurement values. The RMSE takes into account the squares of the differences between the simulation values and the measurement values, sums them up, and then takes the square root to obtain a single value that represents the overall magnitude of the error.

The *MB* and *RMSE* indices are calculated through the following specific formulas. These formulas can precisely quantify these performance measurement indices and help to gain a deeper understanding of the degree to which the model conforms to the actual wind conditions observed by the wind tower.

$$MB = \frac{1}{N}\sum_{i=1}^{n}(M_i - G_i) \tag{6}$$

$$RMSE = \sqrt{\frac{1}{N}\sum_{i=1}^{n}(M_i - G_i)^2} \tag{7}$$

3. Results and Discussions

3.1. Wind Tower Wind Resource Characteristics

In order to conduct an in-depth exploration of the wind energy resources of this wind farm, this subsection first utilizes the complete annual measurements from Tower 8777# in 2010 (with a data completeness rate exceeding 99%) to carry out research on the characteristics of wind resources. **Figure 3** presents the analysis results, showing the wind shear (**Figure 3a**), wind speed, wind direction (**Figure 3b**), and the daily and monthly variations (**Figure 3c,d**) of wind parameters within the project area. As depicted in the boundary-layer wind profile in the project area follows an exponential regular distribution. The comprehensive wind shear index is approximately 0.112, indicating relatively low wind shear. However, below the height of 60 meters above the ground, the wind speed changes rapidly, revealing the complexity of the surface.

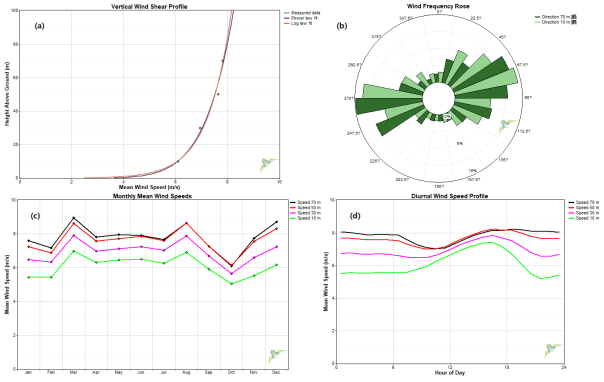

Figure 3. Information on Wind Resource Characteristics of Tower 8777. (**a**) Wind Shear Index; (**b**) Wind Direction; (**c**) Monthly Variations; (**d**) Diurnal Variations.

It can be seen from **Figure 4b** that the main wind directions in this region are northeast by east (NEE) and southwest by west (SWW), which are in line with the east-west oriented canyon topography of the area. The construction of wind farms can achieve higher wind energy utilization efficiency here. In terms of monthly variations, **Figure 4c** shows that the wind speeds are lower in January, February, and October, while they are higher in March, August, and December. Generally speaking, the wind speeds in this region are relatively high in both winter and summer, which is caused by the interaction between the changes in the large-scale westerly circulation and the topography. However, there is no obvious trend in terms of daily variations. After annual statistics, the annual average wind speed is about 8.06 meters per second, indicating relatively good wind energy resources.

Therefore, this comprehensive understanding of the wind conditions in this region not only helps to accurately assess the potential of wind energy utilization but also provides crucial data for the design and optimization of wind-related

projects in the area, ensuring that these projects can adapt well to the local wind environment and providing a powerful verification for the numerical simulation results.

3.2. Model Validation for Wind Resources

The WRF model was used to simulate the hub-height wind speed during the initial construction stage of the research area. The purpose of this simulation is to verify whether the systematic error of the model is within an acceptable range and to conduct further research on this basis. According to the settings of Experiment 1, the wind parameters during the observation period of 2010 at the wind tower were simulated. As shown in **Figure 4a**, when comparing the hourly simulation results with the observed values, there is a high degree of consistency in wind speed, wind direction, and the trend of temporal variation. At a height of 70 meters, the average wind speed deviation is 0.13 m/s (about 1.62%), and the average wind direction deviation is 11.92° (about 6.25%). These results indicate that the systematic error of the numerical model is within 3% (**Table 4**). For Experiment 2, the operation of the Phase I wind farm of the wind power base was incorporated to analyze its impact on the wind field at the location of the wind tower. The results in **Figure 4b** show that the measured wind profile of the wind tower matches well with the simulation results of both Experiment 1 and Experiment 2 and the existing differences may be caused by the systematic error of the model. The results of the two experiments show that the WRF model can effectively simulate the meteorological conditions in the boundary layer of the wind power base in this study. In addition, it also indicates that the construction of the Phase I wind farm has no impact on the meteorological conditions at the wind tower of Phase II of the project. Based on this conclusion, a solid foundation has been laid for the research on the wake effect of the entire wind power base and its interaction with the atmospheric environment after its completion, providing valuable insights for the development and optimization of wind power projects in the area.

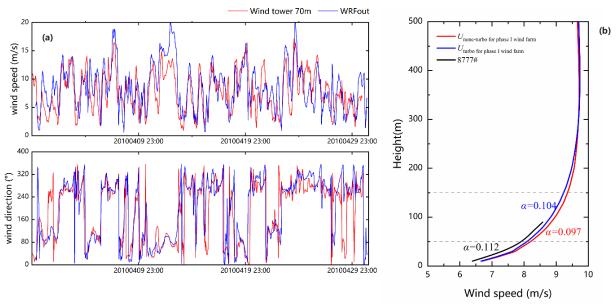

Figure 4. Validation of WRF simulation results with wind tower measurements in (**a**,**b**). (**a**) Time series validation; (**b**) Wind profile comparison (the black line represents the measurements from the meteorological tower, the red line represents the simulation without the wind farm construction, and the blue line represents the simulation after the completion of Phase I of the wind power base).

Table 4. Statistical validation of WRF simulation results against wind tower (8777#) measurements.

Wind Tower	Parameters	MBE	RMSE
8777#	Wind speed	0.13 m/s (1.62%)	1.65 m/s
	Wind direction	11.92° (6.25%)	25.4°

3.3. Analysis of the Interaction between Wind Farms and the Atmospheric Boundary-Layer Environment

Wind power clusters possess a remarkable ability to significantly influence regional atmospheric conditions as they have the potential to modify wind patterns and turbulence levels. When numerous turbines are installed and start operating, they bring about localized modifications in wind speed and direction. These changes, in turn, have a profound impact on atmospheric stability and the dynamics of the boundary layer.

The alterations caused by wind power clusters extend beyond just wind characteristics. They can also have a notable effect on local microclimates. This includes influencing temperature distributions and moisture content, which may subsequently have implications for regional weather patterns. As depicted in **Figure 5**, the results demonstrate that the construction of the wind power base has led to a transformation in the spatial distribution of temperature within the region. Although the differences in temperature distribution before and after construction are relatively minor (as shown in **Figure 5a,b**), the wind power clusters have an impact on regional atmospheric temperatures within the range of −0.5 °C to 0.5 °C. This impact is predominantly concentrated in

the vicinity of the wind farm locations and their adjacent areas, especially in the predominant wind directions, which are the east-west directions in this case. Within the wind power plant area, a significant warming effect is observable (as indicated by the blue area in **Figure 5c**). In contrast, outside this area, a cooling effect prevails (the red area in **Figure 5c**). The presence of the significant warming effect within the wind power plant areas and the cooling effect outside these areas is of utmost importance. These phenomena vividly illustrate how wind farms can affect local climates by changing wind patterns and turbulence levels, thereby influencing the temperature distribution of local microclimates. Such effects hold far-reaching consequences for regional weather patterns, air quality, and the long-term sustainability of energy resources. Hence, conducting in-depth research on the climatic impacts of wind farms is not only essential but also crucial for optimizing their layout and management strategies. This will, in turn, facilitate their sustainable development and seamless integration into environmentally friendly energy systems, ensuring that wind power remains a viable and beneficial energy solution.

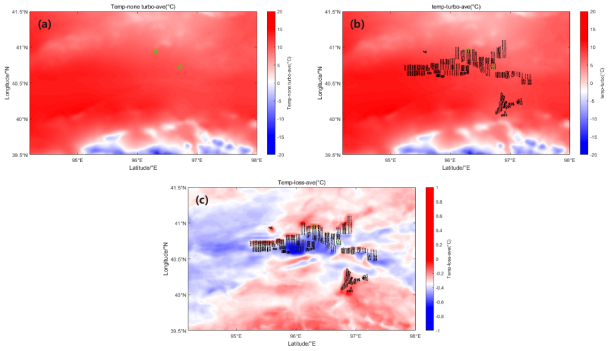

Figure 5. Spatial distributions of temperature fields (a–b, unit: ℃) with and without wind farm construction and their differences (c, unit: ℃). (**a**) The spatial distribution of the temperature field without the influence of the operation of the wind farm; (**b**) The spatial distribution of the temperature field with the influence of the operation of the wind farm; (**c**) The spatial distribution of the differences in the temperature field with and without the influence of the operation of the wind farm.

3.4. Wind Farm Wake Effects

In this study, to better understand these wake effects, based on the simulation results of two control experiments of the coupled WRF and WFP models, the first and second phases of the wind power base were analyzed respectively. **Figure 6** presents in detail the differences in the annual average wind speed before and after the construction of the first-phase wind turbines. The research results clearly show that the wind speed within the wind power base has decreased significantly. In specific areas, this decrease can be as high as 0.8 m/s, and the affected range is relatively wide. In the east-west main wind direction, the affected distance can reach 60–100 km. The reduction in wind speed will seriously affect the performance of the turbines. It may lead to a decrease in the rotational speed of the blades, thereby reducing the power generation capacity of the turbines. In addition, it is surprisingly found that in the construction area of the second-phase project, no significant change in wind speed has been observed. This means that the design and layout of the first-phase wind farm have not yet caused significant disturbances to the wind flow in the area designated for the second-phase project, which is a positive factor for the overall efficiency and productivity of the wind power base. However, whether the construction and operation of the second-phase project will have more far-reaching impacts will be analyzed in the following contents.

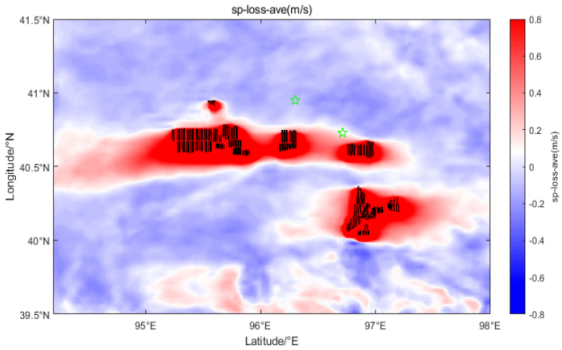

Figure 6. Spatial distribution of wind speed losses in hub height wake effects of Phase I wind farm construction in the large wind power base (unit: m/s). The green pentagon stars represent the locations of two typical wind farms in Phase II of the wind power base.

With the successful completion and full-scale operation of the Phase II wind farms, the entire wind power base has now reached a state of full operation. In combination with the discussion in the previous subsection, this significant situation currently enables a more comprehensive analysis of the wake effects of the wind farm group within this large-scale wind power base system. The numerical simulation results for the year 2022, as shown in **Figure 7a**, provide information that presents the spatial distribution of the wind field before the construction of the wind farms. In this case,

the wind speed within the project area is evenly distributed, approximately 8 m/s, indicating that before the construction of the wind farms, there was originally a relatively stable and consistent wind flow pattern in this region. However, **Figure 7b** shows a stark contrast. It depicts the spatial distribution of the wind field during the construction and operation of the wind farms. It can be seen that compared with the surrounding areas, the wind speed inside the wind farms has decreased significantly. Now, the wind speed within the wind farms ranges from approximately 7.2 to 7.5 m/s. This reduction in wind speed is not only substantial but also has far-reaching implications, and it is significantly lower than the previously assessed wind speed of wind resources, highlighting the significant impact of wind farms on the local wind environment.

Furthermore, **Figure 7c,d** present extremely important information regarding wind speed reduction and its corresponding percentage spatial distribution. These figures vividly reveal an obvious and significant decrease in wind speed both within the wind farm and in its surrounding areas. The range of wind speed reduction is approximately between 0.2 m/s and 0.8 m/s. Expressed as a percentage, this is equivalent to a reduction of about 6% to 10%. Such a significant decrease in wind speed directly affects the performance of the turbines. Since wind speed is a key factor in determining the rotational speed of the turbine blades, a reduction in wind speed will lead to a decrease in the kinetic energy available for conversion into electrical energy, and thus the power generation output will decline. This not only affects the economic benefits of individual turbines but also impacts the overall productivity of the entire wind farm. Therefore, evaluating the wake effects through numerical simulations can provide a reliable scientific basis for the dynamic planning and scientific assessment of the construction plans for wind power bases. Effective simulation methods can ensure that the layout of turbines can minimize the negative impact of wake effects on adjacent turbines. By accurately predicting the variation laws of wake effects, it helps to optimize the layout of wind farms and enables developers and operators to make informed decisions. Moreover, it can also assist in implementing operational strategies that maximize energy production. Essentially, mitigating these wake effects is the key to achieving the dual goals of maximizing energy output and maintaining high overall efficiency within the wind power system.

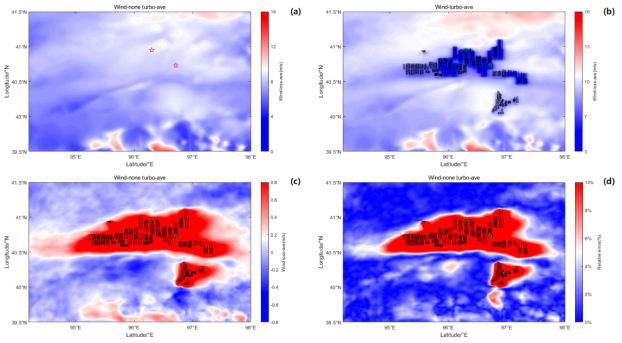

Figure 7. Spatial distributions of wind speed fields (a–b, unit: m/s) with and without wind farm construction and their differences (c, unit: m/s) and loss percentage (d, unit: %). The stars represent the locations of two typical wind farms in Phase II of the wind power base. (**a**) The spatial distribution of the wind field without the influence of the operation of the wind farm; (**b**) The spatial distribution of the wind field with the influence of the operation of the wind farm; (**c**) The spatial distribution of the differences in the wind field with and without the influence of the operation of the wind farm; (**d**) The spatial distribution of the percentage of wind speed loss without the influence of the operation of the wind farm.

4. Conclusions

Considering the profound and multi-faceted effects of complex terrain, this comprehensive study harnesses the power of a mesoscale weather forecasting model that is seamlessly coupled with a wind farm parameterization scheme. This state-of-the-art combination enables highly accurate and detailed numerical simulations of wind resources at the crucial hub height. The focus of this research is to meticulously analyze the wake effects within the large-scale wind power base situated in Jiuquan City, Gansu Province. To ensure a thorough investigation, the research encompasses three sets of meticulously designed control experiments, each corresponding to different construction phases of the wind power base, thereby capturing the dynamic changes in the wind environment over time. The main findings are as follows:

- Data sourced from the 8777# meteorological tower paints a promising picture of the wind conditions in the area. With an annual average wind speed of around 8.06 m/s and predominant wind directions being NEE and SWW, the region showcases excellent potential for wind energy utilization. Moreover, the flat terrain stretching over an extensive area further augments the suitability for developing the wind power base, providing an ideal canvas for wind turbine installation.
- The mesoscale weather forecasting model, which has been

carefully calibrated to account for the complex terrain, has been rigorously validated using meteorological tower data. The results demonstrate a remarkable achievement with a systematic error of less than 3%. This low error range not only validates the model's reliability but also paves the way for more in-depth research, instilling confidence in the subsequent analyses.

- Simulations conducted with the integrated model reveal a fascinating phenomenon. The construction of the wind power base has led to a significant warming effect within the wind farm area. This stands in contrast to the cooling effects observed in the areas outside the wind farm. These temperature variations have implications for the local microclimate and the overall energy balance of the region.
- The analysis of the wake effects has uncovered crucial insights. The first phase of the wind power base construction has had a minimal impact on the second-phase construction area, indicating a well-planned initial layout. During the full-scale operation of the entire wind power base, wind speeds within the wind farm have decreased by approximately 10%. Notably, the influence of the predominant wind direction extends over a substantial distance of more than a hundred kilometers, highlighting the far-reaching consequences of the wind farm's operation on the surrounding wind environment.

Therefore, the study of wake effects within large wind power bases holds a position of utmost significance when it comes to optimizing the design and operation of wind farms. The complex and dynamic nature of wind flow within these large-scale installations demands a comprehensive understanding of how turbines interact with one another. When turbines are in operation, they not only generate power but also have a profound impact on the surrounding wind patterns and turbulence levels. Understanding these interactions is the key to unlocking enhanced efficiency and output for the entire wind farm. By delving into the details of how each turbine affects the wind flow, engineers and researchers can identify optimal turbine placement and spacing. This knowledge can prevent scenarios where the wake of one turbine negatively impacts the performance of adjacent turbines, thereby maximizing the power generation potential of each unit.

This research is not only beneficial for improving the internal functioning of the wind farm but also crucial for minimizing any adverse effects on neighboring turbines. By carefully considering the wake effects, the negative cascading impacts that could potentially spread across the entire wind power base can be mitigated. This, in turn, leads to enhanced energy production as the overall system operates more efficiently. Moreover, such research is fundamental for the sustainable development of wind energy. It ensures that wind power remains a viable and environmentally friendly energy source by optimizing its performance. Additionally, it provides invaluable insights that are essential for dynamic planning and scientific assessment. These insights guide decision-making processes related to expansion, upgrades, and modifications within the wind power project, ultimately contributing to its overall success and seamless integration into the surrounding environment.

Author Contributions

L.Y. and L.B. led the writing of this paper and acknowledged responsibility for the experimental data and results. J.L., H.L. and P.C. drafted the paper, and X.R. and L.Q. led the consolidation of the dataset. This paper is written in cooperation with all of the co-authors. All authors have read and agreed to the published version of the manuscript.

Funding

This research was funded by "The Factors Affecting the Accuracy of Wind Resource Assessment and Comprehensive Post-Evaluation Techniques for Operating Wind Power Projects," grant number YJ24.002; "The Research and Application of Future Medium to Long Term Wind Resource Assessment for Wind Farms Based on Artificial Intelligence Project," grant number 2023021. The article publishing charge (APC) is funded by the Haizhuang Wind Power Co., Ltd., China State Shipbuilding Corp (CSSC).

Institutional Review Board Statement

Not applicable.

Informed Consent Statement

Not applicable.

Data Availability Statement

The publicly available data used in this study have been acknowledged in the Acknowledgments section. By copyright requirements, the measured data used in this study can be obtained by contacting the authors.

Acknowledgments

We are grateful for the ERA5 reanalysis datasets provided by the European Centre for Medi-um-Range Weather Forecasts (ECMWF), https://www.ecmwf.int/ (accessed on 10 October 2024). The land cover classification data are sourced from the University of Maryland (UMD) Land Cover Classification Scheme based on MODIS data and other auxiliary data, https://glad.umd.edu/ (accessed on 10 October 2024). The measurements of the wind tower are from Haizhuang Wind Power Co., Ltd., China State Shipbuilding Corp (CSSC), https://www.csschz.com/?en/ (accessed on 10 October 2024). The authors would like to thank all their colleagues at the observation stations on the TP for maintaining the instruments.

Conflict of Interest

The authors declare no conflict of interest.

References

[1] IEA, 2014. China Wind Energy Development Roadmap 2050. OECD Publishing: Paris, France.

[2] Wang, Q., Luo, K., Wu, C., et al., 2022. Mesoscale Simulations of A Real Onshore Wind Power Base in Complex Terrain: Wind Farm Wake Behavior and Power Production. Energy. 241. DOI: https://doi.org/10.1016/j.energy.2021.122873

[3] Harris, R., Zhou, L., Xia, G. Satellite Observations of Wind Farm Impacts on Nocturnal Land Surface Temperature in Iowa. Remote Sensing., 6(12), 12234–46. DOI: https://doi.org/10.3390/rs61212234

[4] Chen, S., Cao, R., Xie, Y., 2021. Study of the Seasonal Variation in Aeolus Wind Product Performance over China using ERA5 and Radiosonde Data. Atmospheric Chemistry and Physics,. 21(15), 11489–11504. DOI: https://doi.org/10.5194/acp-21-11489-2021

[5] De Montera, L., Berger, H., Husson, R., et al., 2022. High-resolution Offshore Wind Resource Assessment at Turbine Hub Height with Sentinel-1 Synthetic Aperture Radar (SAR) Data and Machine Learning. Wind Energy Science. 7(4), 1441–1453. DOI: https://doi.org/10.5194/wes-7-1441-2022

[6] Abkar, M., Porté-Agel, F., The Effect of Free-Atmosphere Stratification on Boundary-layer Flow and Power Output from Very Large Wind Farms. Energies. 6(5), 2338–61. DOI: https://doi.org/10.3390/en6052338

[7] Mears, C., Lee, T., Ricciardulli, L., et al., 2022. Improving the Accuracy of the Cross-Calibrated Multi-Platform (CCMP) Ocean Vector Winds. Remote Sensing. 14, 4230. DOI: https://doi.org/10.3390/rs14174230

[8] Keith, D.W., DeCarolis, J.F., Denkenberger, D.C., et al., 2004. The Influence of Large-scale Wind Power on Global Climate. Proceedings of the National Academy of Sciences of the United States of America (PNAS), 101(46), 16115–20. DOI: https://doi.org/10.1073/pnas.0406930101

[9] Porté-Agel, F., Lu, H., Wu, Y.T., 2014. Interaction between Large Wind Farms and the Atmospheric Boundary Layer. Procedia IUTAM. 10, 307–318. DOI: https://doi.org/10.1016/j.piutam.2014.01.026

[10] Churchfield, M.J., Lee, S., Michalakes, J., et al., 2012. A Numerical Study of the Effects of Atmospheric and Wake Turbulence on Wind Turbine Dynamics. Journal of Turbulence, 13, 1–32. DOI: https://doi.org/10.1080/14685248.2012.668191

[11] Skamarock, W.C., Klemp, J.B., Dudhia, J., 2008. A Description of the Advanced Research WRF Version 3.0 (NCAR TECHNICAL NOTE). Available from: https://www.researchgate.net/publication/306154004_A_Description_of_the_Advanced_Research_WRF_Version_3 (cited on 10 October 2022).

[12] Wang, Q., Luo, K., Yuan, R., et al., 2020. A Multiscale Numerical Framework Coupled with Control Strategies for Simulating A Wind Farm in Complex Terrain. Energy. 203. DOI: https://doi.org/10.1016/j.energy.2020.117913

[13] Carvalho, D., Rocha, A., Santos, C.S., et al., 2013. Wind Resource Modeling in Complex Terrain Using Different Mesoscale–microscale Coupling Techniques. Applied Energy, 108, 493–504. DOI: https://doi.org/10.1016/j.apenergy.2013.03.074

[14] Srinivas, C.V., Yesubabu, V., Hari Prasad, D., et al., 2018. Simulation of An Extreme Heavy Rainfall Event over Chennai, India using WRF: Sensitivity to Grid Resolution and Boundary Layer Physics. Atmospheric Research, 210, 66–82. DOI: https://doi.org/10.1016/j.atmosres.2018.04.014

[15] Fitch, A.C., Olson, J.B., Lundquist, J.K. Parameterization of Wind Farms in Climate Models. Journal of Climate, 26(17), 6439–58. DOI: https://doi.org/10.1175/JCLI-D-12-00376.1

[16] Abkar, M., Porté-Agel, F., A New Wind-farm Parameterization for Large-scale Atmospheric Models. Journal

of Renewable and Sustainable Energy, 7(1), 013121. DOI: https://doi.org/10.1063/1.4907600

[17] Baidya Roy, S. Simulating Impacts of Wind Farms on Local Hydrometeorology. Journal of Wind Engineering and Industrial Aerodynamics, 99(4), 491–498. DOI: https://doi.org/10.1016/j.jweia.2010.12.013

[18] Mughal, M.O., Lynch, M., Yu, F., et al., 2017. Wind Modeling, Validation and Sensitivity Study Using Weather Research and Forecasting Model in Complex Terrain. Environmental Modelling & Software, 90, 107–125. DOI: https://doi.org/10.1016/j.envsoft.2017.01.009

[19] Malardel, S., Wedi, N., Deconinck, W., et al., 2015. A New Grid for the IFS from Newsletter No.146–Winter. Available from: https://www.ecmwf.int/sites/default/files/elibrary/2016/17262-new-grid-ifs.pdf (cited on 10 October 2022).

[20] Janjic, Z.I., 1994. The Step-mountain Eta Coordinate Model: Further Developments of the Convection, Viscous Sublayer, and Turbulence Closure Schemes. Monthly Weather Review, 122, 927–945. DOI: https://doi.org/10.1175/1520-0493(1994)122<0927:TSMECM>2.0.CO;2

[21] Grell, G.A. Prognostic Evaluation of Assumptions Used by Cumulus Parameterizations. Monthly Weather Review, 121, 764–787. DOI: https://doi.org/10.1175/1520-0493(1993)121<0764:PEOAUB>2.0.CO;2

[22] Grell, G.A., Devenyi, D., 2002. A Generalized Approach to Parameterizing Convection Combining Ensemble and Data Assimilation Techniques. Geophysical Research Letters , 29, 38–31. DOI: https://doi.org/10.1029/2002GL015311

[23] Thompson, G., Field, P.R., Rasmussen, R.M., et al., 2008. Explicit Forecasts of Winter Precipitation Using An Improved Bulk Microphysics Scheme. Part II: Implementation of A New Snow Parameterization. Monthly Weather Review, 136, 5095–5115. DOI: https://doi.org/10.1175/2008MWR2387.1

[24] Mlawer, E.J., Taubman, S.J., Brown, P.D., et al., 1997. Radiative Transfer for Inhomogeneous Atmospheres: RRTM, A Validated Correlated-K model for the Longwave. Journal of Geophysical Research: Atmospheres, 102, 16663–16682. DOI: https://doi.org/10.1029/97jd00237

[25] Dudhia, J. Numerical Study of Convection Observed during the Winter Monsoon Experiment Using A Mesoscale Two-dimensional Model. Journal of the Atmospheric Sciences, 46, 3077–3107. DOI: https://doi.org/10.1175/1520-0469(1989)046<3077:NSOCOD>2.0.CO;2

[26] Tewari, M., Chen, F., Wang, W., et al., 2004. Implementation and Verification of the Unified NOAH Land Surface Model in the WRF Model. Bulletin of the American Meteorological Society, 2165–2170.

[27] Beljaars, A.C.M., Brown, A.R., Wood, N. A New Parametrization of Turbulent Orographic Form Drags. Quarterly Journal of the Royal Meteorological Society, 130(599), 1327–1347. DOI: https://doi.org/10.1256/qj.03.73

[28] Zhou, X., Yang, K., Ouyang, L., et al., 2021. The Added Value of Kilometer-scale Modeling over the Third Pole Region: a CORDEX-CPTP Pilot Study. Climate Dynamics, 57(7–8), 1673–1687. DOI: https://doi.org/10.1007/s00382-021-05653-8

[29] Fitch, A.C., Olson, J.B., Lundquist, J.K., et al., 2012. Local and Mesoscale Impacts of Wind Farms as Parameterized in A Mesoscale NWP Model. Monthly Weather Review, 140(9), 3017–3038. DOI: https://doi.org/10.1175/MWR-D-11-00352.1